CHAPTER 2

X-RAY FLUORESCENCE TECHNIQUE

2.1 Introduction

X-ray fluorescence (XRF) technique has been widely used for elemental analysis not only in the laboratory but also in the field. This technique can be done rapidly and nondestructively over a wide range of elemental concentration.

In XRF analysis, the sample is exposed to photons (γ-or X-rays) or charged particles (usually protons and electrons) which cause the sample atoms to fluoresce. The energies of these fluorescent X-rays are characteristic of the atomic number (Z) of the atoms excited; hence the concentrations of specific elements can be determined from measurements of the intensities of their respective fluorescent X-rays.

2.2 Basic Principles[1, 2, 3, 4, 5]

When a charged particle or a photon interacts with an atom, several phenomena may take place. If the particle or photon had sufficient energy, an electron in the inner shell

(K or L) may be ejected from the atom resulting in the creation of an electron hole. The hole will be filled by an electron from the outer shell which has higher energy and the extra energy is emitted as a fluorescent X-ray or so called a characteristic X-ray.

Let E_o = energy level of the electron from the outer shell,

E_i = energy of the inner shell where the electron hole is created,

and E_x = energy of the fluorescent X-ray.

Thus $E_x = E_o - E_i$.

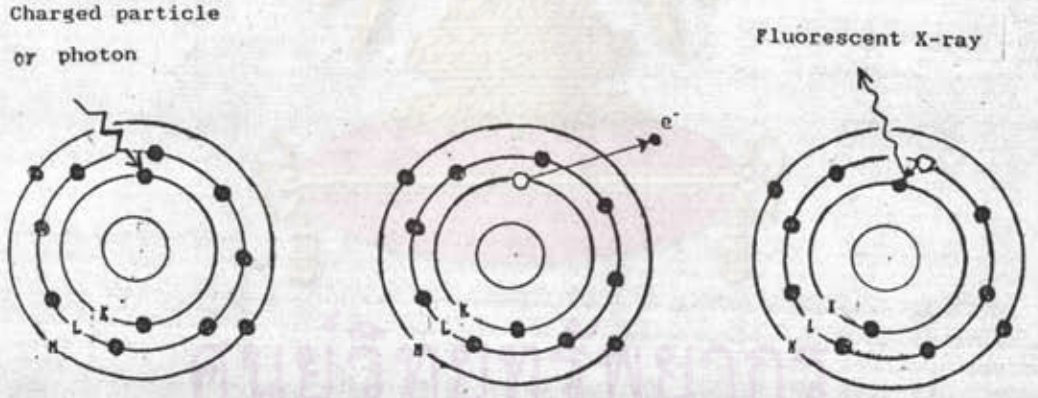

(i) Interaction of charged particle or photon with an atomic electron

(ii) Ejection of an atomic electron

(iii) Electronic transition and emission of fluorescent X-ray

Fig 2.1 Emission of fluorescent X-ray.

The life time of the K and L hole varies between 10^{-9} and 10^{-16}second. The different X-ray groups are labelled by capital letters corresponding to the shell with electron vacancies and suffixed for the electrons which drop into the vacancies (K_α, K_β, L_α, L_β, L_γ, etc.). The number of X-ray groups with different energies is very large, corresponding to the various combinations of atomic electron shells and subshells. Figure 2.2 shows the electronic energy level diagram with the origin of the main lines in the K and L X-ray series.

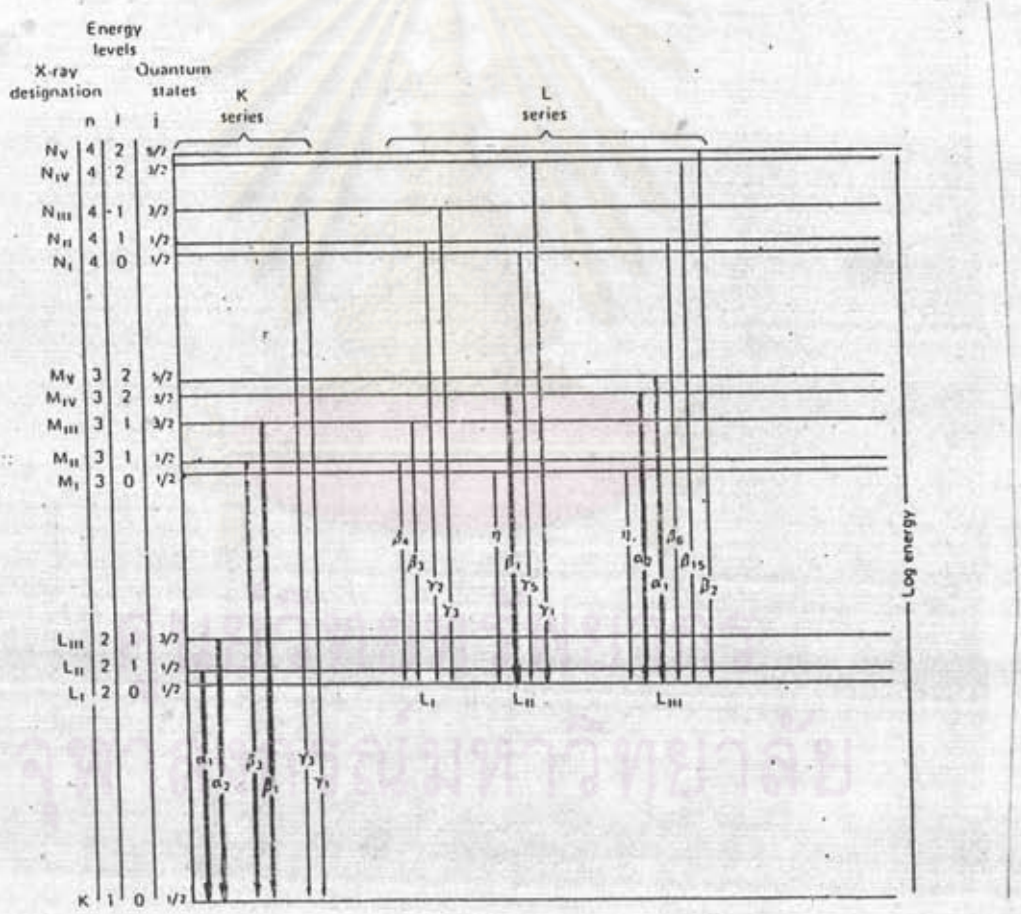

Fig 2.2 Partial energy level diagram showing the origin of the main lines in the K and L X-ray series.

The energy of an X-ray line is characteristic for each of the elements, and increases with increasing atomic number as can be seen in Table 2.1. The energies of K and L X-ray are in the ranges of about 50 eV - 140 keV and 350 eV - 20 keV respectively. In practice, the energies from 1 keV up to 100 keV are usually involved in XRF analysis.

To eject a K or an L electron from an atom, the incident photon or charged particle must overcome the binding energy between the electron and the nucleus i.e. K_{ab} or L_{ab} as tabulated in Table 2.1. Therefore, the incident photon must have an energy equal to or greater than K_{ab} or L_{ab} in order to knock a K or L electron out of its atom. The L_{Iab}, L_{IIab} and L_{IIIab} are the binding energies of L electrons in subshell I, II and III respectively.

Table 2.1: X-Ray Critical Absorption and Emission Energies in keV.

Atomic Number	Element	K series					L series							
		K_{ab}	$K\beta_1$	$K\beta_3$	$K\alpha_1$	$K\alpha_2$	I_{Lab}	L_{IIab}	L_{IIIab}	$L\gamma_1$	$L\beta_1$	$L\beta_1$	$L\alpha_1$	$L\alpha_2$
1	Hydrogen	0.0136‡												
2	Helium	0.0246‡												
3	Lithium	0.055				0.052								
4	Beryllium	0.116§				0.110								
5	Boron	0.192†				0.185								
6	Carbon	0.283				0.282								
7	Nitrogen	0.399				0.392								
8	Oxygen	0.531				0.523								
9	Fluorine	0.687†				0.677								
10	Neon	0.874*				0.851§	0.048†	0.022†	0.022†					
11	Sodium	1.08*		1.067		1.041	0.055§	0.034§	0.034§					
12	Magnesium	1.303		1.297		1.254	0.063	0.050	0.049					
13	Aluminum	1.559		1.553	1.487	1.486	0.087	0.073**	0.072**					
14	Silicon	1.838		1.832	1.740	1.739	0.118*	0.099**	0.098**					
15	Phosphorus	2.142		2.136	2.015§	2.014§	0.153*	0.129§	0.128§					
16	Sulphur	2.470		2.464	2.308	2.306	0.193*	0.164**	0.163**					
17	Chlorine	2.819¶		2.815	2.622	2.621	0.238*	0.203§	0.202§					
18	Argon	3.203		3.192§	2.957	2.955	0.287*	0.247**	0.245**					
19	Potassium	3.607		3.589	3.313	3.310	0.341*	0.297**	0.294**					
20	Calcium	4.038		4.012	3.691	3.688	0.399*	0.352	0.349			0.344		0.341
21	Scandium	4.496		4.460	4.090	4.085	0.462*	0.411**	0.406**			0.399		0.395
22	Titanium	4.964		−4.931	4.510	4.504	0.530*	0.460**	0.454**			0.458		0.452
23	Vanadium	5.463		−5.427	4.952	4.944	0.604*	0.519**	0.512**			0.519		0.510
24	Chromium	5.988		−5.946	5.414	5.405	0.679*	0.583**	0.574**			0.581		0.571
25	Manganese	6.537		6.490	5.898	5.887	0.762*	0.650**	0.639**			0.647		0.636
26	Iron	7.111		7.057	6.403	6.390	0.849*	0.721**	0.708**			0.717		0.704
27	Cobalt	7.709		7.649	6.930	6.915	0.929*	0.794**	0.779**			0.790		0.775
28	Nickel	8.331	8.328	8.264	7.477	7.460	1.015*	0.871**	0.853**			0.866		0.849
29	Copper	8.980	8.976	8.904	8.047	8.027	1.100*	0.953	0.933			0.948		0.928
30	Zinc	9.660	9.657	9.571	8.638	8.615	1.200*	1.045	1.022			1.032		1.009

Atomic Number	Element	K series					L series							
		K_{ab}	$K\beta_2$	$K\beta_1$	$K\alpha_1$	$K\alpha_2$	L_{1ab}	L_{11ab}	L_{111ab}	$L\gamma_1$	$L\beta_2$	$L\beta_1$	$L\alpha_1$	$L\alpha_2$
31	Gallium	10.368	10.365	10.263	9.251	9.234	1.30*	1.134**	1.117**			1.122	1.096	
32	Germanium	11.103	11.100	10.981	9.885	9.854	1.42*	1.248**	1.217**			1.216	1.186	
33	Arsenic	11.863	11.863	11.725	10.543	10.507	1.529	1.359	1.323			1.317	1.282	
34	Selenium	12.652	12.651	12.495	11.221	11.181	1.652	1.473	1.434			1.419	1.379	
35	Bromine	13.475	13.465	13.290	11.923	11.877	1.794§	1.599**	1.552**			1.526	1.480	
36	Krypton	14.323	14.313	14.112	12.648	12.597	1.931§	1.727**	1.675**			1.638§	1.587**	
37	Rubidium	15.201	15.184	14.960	13.394	13.335	2.067	1.866	1.806			1.752	1.694	1.692
38	Strontium	16.106	16.083	15.834	14.164	14.097	2.221	2.008	1.941			1.872	1.806	1.805
39	Yttrium	17.037	17.011	16.736	14.957	14.882	2.369	2.154	2.079			1.996	1.922	1.920
40	Zirconium	17.998	17.969	17.666	15.774	15.690	2.547	2.305	2.220	2.302	2.219	2.124	2.042	2.040
41	Niobium	18.987	18.951	18.621	16.614	16.520	2.706	2.467**	2.374	2.462	2.367	2.257	2.166	2.163
42	Molybdenum	20.002	19.964	19.607	17.478	17.373	2.884	2.627	2.523	2.623	2.518	2.395	2.293	2.290
43	Technetium	21.054§	21.012§	−20.585¶	18.410¶	18.328¶	3.054§	2.795§	2.677§	2.792§	2.674§	2.538§	2.424§	2.420§
44	Ruthenium	22.118	22.072	21.655	19.278	19.149	3.236§	2.966	2.837	2.964	2.836	2.683	2.558	2.554
45	Rhodium	23.224	23.169	22.721	20.214	20.072	3.419	3.145	3.002	3.144	3.001	2.834	2.696	2.692
46	Palladium	24.347	24.297	23.816	21.175	21.018	3.617	3.329	3.172	3.328	3.172	2.990	2.838	2.833
47	Silver	25.517	25.454	24.942	22.162	21.988	3.810	3.528	3.352	3.519	3.348	3.151	2.984	2.978
48	Cadmium	26.712	26.641	26.093	23.172	22.982	4.019	3.727	3.538	3.716	3.528	3.316	3.133	3.127
49	Indium	27.928	27.859	27.274	24.207	24.000	4.237	3.939	3.729	3.920	3.713	3.487	3.287	3.279
50	Tin	29.190	29.106	28.483	25.270	25.042	4.464	4.157	3.928	4.131	3.904	3.662	3.444	3.435
51	Antimony	30.486	30.387	29.723	26.357	26.109	4.697	4.381	4.132	4.347	4.100	3.843	3.605	3.595
52	Tellurium	31.809	31.698	30.993	27.471	27.200	4.938	4.613	4.341	4.570	4.301	4.029	3.769	3.758
53	Iodine	33.164	33.016	32.292	28.610	28.315	5.190	4.856	4.559	4.800	4.507	4.220	3.937	3.926
54	Xenon	34.579	34.446¶	33.644	29.802¶	29.485¶	5.452	5.104	4.782	5.036§	4.720§	4.422§	4.111§	4.098§
55	Cesium	35.959	35.819	34.984	30.970	30.623	5.720	5.358	5.011	5.280	4.936	4.620	4.286	4.272
56	Barium	37.410	37.255	36.376	32.191	31.815	5.995	5.623	5.247	5.531	5.156	4.828	4.467	4.451
57	Lanthanum	38.931	38.728	37.799	33.440	33.033	6.283	5.894	5.489	5.789	5.384	5.043	4.651	4.635
58	Cerium	40.449	40.231	39.255	34.717	34.276	6.561	6.165†	5.729	6.052	5.613	5.262	4.840	4.823
59	Praseodymium	41.998	41.772	40.746	36.023	35.548	6.846	6.443	5.968	6.322	5.850	5.489	5.034	5.014
60	Neodymium	43.571	43.298¶	42.269	37.359	36.845	7.144	6.727	6.215	6.602	6.090	5.722	5.230	5.208
61	Promethium	45.207§	44.955§	−43.945¶	38.649¶	38.160¶	7.448§	7.018§	6.466§	6.891§	6.336§	5.956	5.431	5.408§
62	Samarium	46.846	46.553¶	45.400	40.124	39.523	7.754	7.281¶	6.721	7.180	6.587	6.206	5.636	5.609
63	Europium	48.515	48.241	47.027	41.529	40.877	8.069	7.624	6.983	7.478	6.842	6.456	5.846	5.816
64	Gadolinium	50.229	49.961	48.718	42.983	42.280	8.393	7.940	7.252	7.788	7.102	6.714	6.059	6.027
65	Terbium	51.998	51.737	50.391	44.470	43.737	8.724	8.258	7.519	8.104	7.368	6.979	6.275	6.241
66	Dysprosium	53.789	53.491	52.178	45.985	45.193	9.083	8.621¶	7.850¶	8.418	7.638	7.249	6.495	6.457
67	Holmium	55.615	55.292**	53.934§	47.528	46.686	9.411	8.920	8.074	8.748	7.912	7.528	6.720	6.680
68	Erbium	57.483	57.088	55.690	49.099	48.205	9.776	9.263	8.364	9.089	8.188	7.810	6.948	6.904
69	Thulium	59.335¶	58.969**	57.576¶	50.730	49.762	10.144	9.628	8.652	9.424	8.472	8.103	7.181	7.135
70	Ytterbium	61.303	60.959	59.352	52.360	51.326	10.486	9.977	8.943	9.779	8.758	8.401	7.414	7.367
71	Lutecium	63.304	62.946	61.282	54.063	52.959	10.867	10.345	9.241	10.142	9.048	8.708	7.654	7.604
72	Hafnium	65.313	64.936	63.209	55.757	54.579	11.264	10.734	9.556	10.514	9.346	9.021	7.898	7.843
73	Tantalum	67.400	66.999	65.210	57.524	56.270	11.676	11.130	9.876	10.892	9.649	9.341	8.145	8.087
74	Tungsten	69.508	69.090	67.233	59.310	57.973	12.090	11.535	10.198	11.283	9.959	9.670	8.396	8.333
75	Rhenium	71.662	71.220	69.298	61.131	59.707	12.522	11.955	10.531	11.684	10.273	10.008	8.651	8.584
76	Osmium	73.860	73.393	71.404	62.991	61.477	12.965	12.383	10.869	12.094	10.596	10.354	8.910	8.840
77	Iridium	76.097	75.605	73.549	64.886	63.278	13.413	12.819	11.211	12.509	10.918	10.706	9.173	9.098
78	Platinum	78.379	77.866	75.736	66.820	65.111	13.873	13.268	11.559	12.939	11.249	11.069	9.441	9.360
79	Gold	80.713	80.165	77.968	68.794	66.980	14.353	13.733	11.919	13.379	11.582	11.439	9.711	9.625
80	Mercury	83.106	82.526	80.258	70.821	68.894	14.841	14.212	12.285	13.828	11.923	11.823	9.987	9.896
81	Thallium	85.517	84.904	82.558	72.860	70.820	15.346	14.697	12.657	14.288	12.268	12.210	10.266	10.170
82	Lead	88.001	87.343	84.922	74.957	72.794	15.870	15.207	13.044	14.762	12.620	12.611	10.549	10.448
83	Bismuth	90.521	89.833	87.335	77.097	74.805	16.393	15.716	13.424	15.244	12.977	13.021	10.836	10.729
84	Polonium	93.112	92.386	89.809	79.296	76.868	16.935	16.244	13.817	15.740	13.338	13.441	11.128	11.014
85	Astatine	95.740	94.976	92.319	81.525	78.956	17.490	16.784	14.215	16.248	13.705	13.873	11.424	11.304
86	Radon	98.418	97.616	94.877	83.800	81.080	18.058	17.337	14.618	16.768	14.077	14.316	11.724	11.597
87	Francium	101.147	100.305	97.483	86.119	83.243	18.638	17.904	15.028	17.301	14.459	14.770	12.029	11.894
88	Radium	103.927	103.048	100.136	88.485	85.446	19.233	18.481	15.442	17.845	14.839	15.233	12.338	12.194
89	Actinium	106.759	105.838	102.846	90.894	87.681	19.842	19.078	15.865	18.405	15.227	15.712	12.650	12.499
90	Thorium	109.630	108.671	105.592	93.334	89.942	20.460	19.688	16.296	18.977	15.620	16.200	12.966	12.808
91	Protactinium	112.581	111.575	108.408	95.851	92.271	21.102	20.311	16.731	19.559	16.022	16.700	13.291	13.120
92	Uranium	115.591	114.549	111.289	98.428	94.648	21.753	20.943	17.163	20.163	16.425	17.218	13.613	13.438
93	Neptunium	118.619	117.533	114.181	101.005	97.023	22.417	21.596	17.614	20.774	16.837	17.740	13.945	13.758
94	Plutonium	121.720	120.592	117.146	103.653	99.457	23.097	22.262	18.066	21.401	17.254	18.278	14.279	14.082
95	Americium	124.876	123.706	120.163	106.351	101.932	23.793	22.944	18.525	22.042	17.677	18.829	14.618	14.411
96	Curium	128.088	126.875	123.235	109.098	104.448	24.503	23.640	18.990	22.699	18.106	19.393	14.961	14.743
97	Berkelium	131.357	130.101	126.362	111.896	107.023	25.230	24.352	19.461	23.370	18.540	19.971	15.309	15.079
98	Californium	134.683	133.383	129.544	114.745	109.603	25.971	25.080	19.938	24.056	18.980	20.562	15.661	15.420
99		138.067	136.724	132.781	117.646	112.244	26.729	25.824	20.422	24.758	19.426	21.166	16.018	15.764
100		141.510	140.122	136.075	120.598	114.926	27.503	26.584	20.912	25.475	19.879	21.785	16.379	16.113

For $Z \leq 69$, values without symbols are derived from (*1*). Values prefixed with a − sign are $K\beta_{1ab}$.

For $Z \geq 70$, absorption-edge values are from (*1*) in the case of Z = 70–83, 88, 90, and 92; remaining absorption edges to Z = 100 are obtained from these by least-squares quadratic fitting. All emission values for $Z \geq 70$ are derived from the preceding absorption edges, and others based on (*4*), using the transition relations $K\alpha_1 = K_{ab} - L_{111}$, $K\alpha_2 = K_{ab} - L_{11}$, $K\beta_1 = K_{ab} - M_{111}$, etc.

* Obtained from R. D. Hill, E. I. Church, J. W. Mihelich (*3*). † Derived from Compton and Allison (*2*). ‡ Derived from C. E. Moore (*3*).

¶ Values derived from Cauchois and Hulubei (*1*) which deviate from the Moseley law. Better-fitting values are: Z = 17, K_{ab} = 2.826; Z = 43, $K\alpha_1$ = 18.370, $K\alpha_2$ = 18.250, $K\beta_1$ = 20.612; Z = 54, $K\alpha_1$ = 29.779, $K\alpha_2$ = 29.463, $K\beta_1$ = 34.398; Z = 60, $K\beta_1$ = 43.349; Z = 61, $K\alpha_1$ = 38.726, $K\alpha_2$ = 38.180, $K\beta_1$ = 43.811; Z = 62, $K\beta_1$ = 46.581, L_{11} = 7.312; Z = 66, L_{11} = 8.591, L_{111} = 7.790; Z = 69, K_{ab} = 59.382, $K\beta_1$ = 57.487.

§ Calculated by method of least squares. ** Calculated by transition relations.

2.2.1 Selection Rules

According to the quantum mechanics theory, the transition of an electron from an outer shell to an electron hole in the inner shell obeys the following "selection rules":

$$\Delta n \geq 1,$$

$$\Delta l = \pm 1,$$

$$\Delta j = \pm 1 \text{ or } 0,$$

where n is the principal quantum number,

l is the angular quantum number,

j is the total angular moment (angular plus, spin),

hence $j = l \pm \frac{1}{2}$.

The possible electronic transitions can also be seen in Fig. 2.2 corresponding to the selection rules. The transition between K shell and L_I is an example of a forbidden transition because $\Delta l \neq \pm 1$

In practice, when a beam of photons or charged particles strikes the sample, a number of electron holes will be created in the sample atoms. The emission of each X-ray line depends upon:

(i) the probability that the incident photons will ionize an atom in that subshell;

(ii) the probability that the electron hole created in that subshell will be filled by an electron from a particular subshell;

(iii) the probability that the emitted fluorescent X-ray will leave the atom without being absorbed within the atom itself.

For example, the most probable (most intense) K X-ray line, i.e. $K\alpha_1$ is emitted by the transition of electron from L_{III} to K. The probability of emission $K\alpha_2$ X-ray line (L_{II} to K) is only about 50 % of the $K\alpha_1$ line. The thick lines in Fig. 2.2 indicate these two most intense lines.

The fluorescent X-ray may be absorbed by an outer electron of the atom resulting in its ejection from the atom. This phenomenon is known as "Auger effect" and the ejected electron is called the "Auger electron."

Let ω = fluorescence yield,

n_f = the number of fluorescent X-rays that effectively leave the atom in a period of time,

and n = the number of electron holes formed in a period of time.

Thus, the fluorescence yield is defined by

$$\omega = \frac{n_f}{n}$$

For example, the K fluorescence yield(ω_K) equals the number of K X-rays emitted devided by the number of electron holes formed in K shell (n_K). Hence

$$\omega_K = \frac{n_f(K\alpha_1) + n_f(K\alpha_2) + n_f(K\beta_1) + \ldots}{n_K}$$

where $n_f(K\alpha_1)$, $n_f(K\alpha_2)$, $n_f(K\beta_1)$,...are the number of $K\alpha_1$, $K\alpha_2$, $K\beta_1$, ...X-ray lines emitted.

As there are only two competitive phenomena, the Auger effect yield can be defined by $1 - \omega$.

The fluorescence yield increases with increasing atomic number and ω_K is much larger than ω_L, and ω_L is much larger than ω_M as can be seen in Fig. 2.3

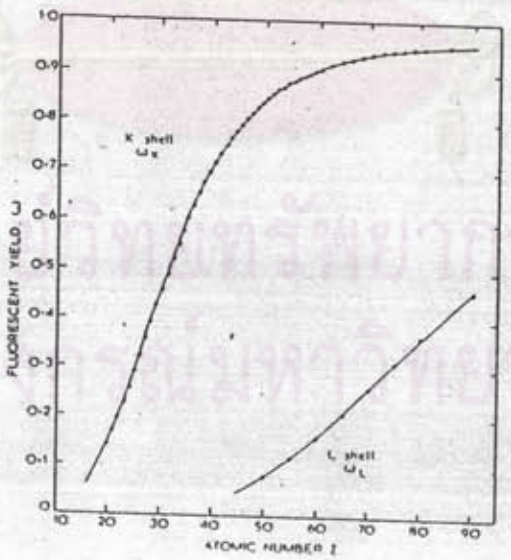

Fig 2.3 The relation between the fluorescence yield and the atomic number

2.3 Elemental Analysis with Radioisotope Excited XRF Spectrometer.

2.3.1 Intensity of Fluorescent X-rays

The basic principles of X-ray fluorescence (XRF) analysis are given below.

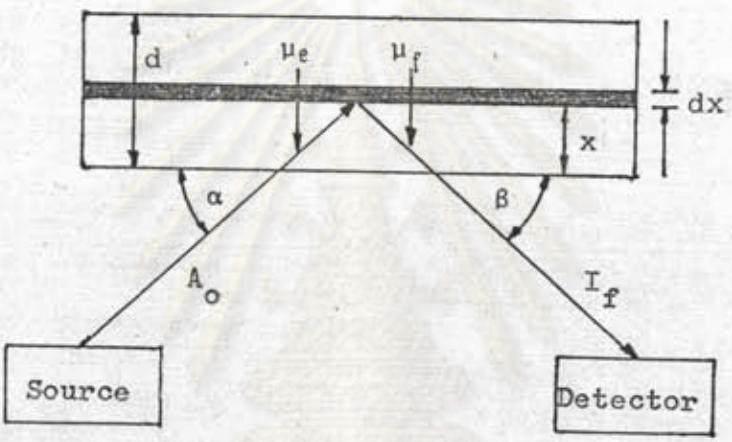

Fig. 2.4 Scheme for derivation of the X-ray fluorescence equation.

Fig. 2.4 shows X-rays incident on a sample interacting in a layer dx at a distance x from the sample surface, and the intensity dI_f (counts/sec) of characteristic X-rays which are detected with overall efficiency k (including the geometrical efficiency G and the detector efficiency η , i.e., $k = G \cdot \eta$) is given by:

$$dI_f = k\Lambda_o \omega \tau C_A \rho \exp\left[-\mu_e \frac{\rho x}{\sin \alpha}\right] \exp\left[-\mu_f \frac{\rho x}{\sin \beta}\right] dx$$

where A_o = source output, photon/sec,

ω = fluorescence yield of the element for K and L X-rays, respectively,

τ = photoelectric mass absorption coefficient of the element, cm^2/g, at the incident energy,

$\omega\tau$ = X-ray excitation cross-section,

C_A = weight concentration of the element A to be analyzed in the sample,

ρ = density of the sample material, g/cm^3,

μ_e, μ_f = mass absorption coefficient of the sample material for the primary (incident) radiation, and for the excited (fluorescent) radiation cm^2/g, respectively,

α, β = angles between the sample surface and the incident radiation and the fluorescent radiation, respectively.

By integrating for a specimen of thickness d (i.e., between x=0 and x=d) the general expression follows:

$$I_f = \frac{k\, A_o \omega\tau C_A}{\mu_e + \frac{\sin\alpha}{\sin\beta}\mu_f}\left[1-\exp-\left(\frac{\mu_e}{\sin\alpha}+\frac{\mu_f}{\sin\beta}\right)\rho d\right]$$

Inspite of a wide range of incident and emitted angles for central and annular source geometries it can be

safely assumed that the radiation enters and leaves the sample normally. Therefore, I_f can be approximated by

$$I_f = \frac{kA_o\omega\tau C_A}{\mu_e+\mu_f}\left[1-\exp-(\mu_e+\mu_f)\rho d\right]$$

The exponential term will rapidly decrease with increasing thickness d of the sample layer. As a consequence the saturation depth d_s is given by

$$d_s = \frac{3}{\rho(\mu_e+\mu_f)}$$

which corresponds to 95% of the counts of an infinite sample layer often reached in practice. In these cases, the simplified expression of I_f holds:

$$I_f = K\frac{C_A}{\mu_e+\mu_f}$$

with $K = kA_o\omega\tau$

From the above equation, it follows that the fluorescent intensity of an element to be analyzed depends not only on the concentration C_A but also on the absorption characteristics of the sample, i.e. on the mass absorption coefficients of the specimen for both the incident and fluorescent radiation. Therefore, because other elements of a

sample affect these coefficients, the relationship between fluorescent intensity and weight concentration is generally linear in samples.

It is also necessary to consider the two types of scattered radiation, namely: "Coherent scattered radiation" and "Incoherent scattered radiation." Only the mass absorption coefficient for the incident radiation must be considered because of the equal energies of the incident and coherent scattered radiations. The intensity is thus given by

$$I_c = \frac{k_s A_o \sigma_c}{2\mu_e}[\, 1 - \exp - (2\mu_e \rho d)]$$

where σ_c - coherent scatter cross-section of the sample material at the incident energy,

k_s - overall efficiency for the scattered radiation,

For the incoherent scattered radiation or the compton radiation, its intensity is

$$I_{ic} = \frac{k_s A_o \sigma_{ic}}{\mu_e + \mu_{ic}}[\, 1 - \exp - (\mu_e + \mu_{ic})\, \rho d]$$

where σ_{ic} - compton (incoherent) scatter cross-section at the incident energy,

μ_{ic} - mass absorption coefficient of the sample material for the incoherent scattered radiation with an energy, being lost as a result of an inelastic scattering process.

From the relationship between the fluorescent radiation and the scattered radiation, an estimation of the signal-to-background ratio is possible. For instance, for infinitely thick samples, it follows approximately that

$$\left[\frac{I_f}{I_c + I_{ic}}\right]_{thick} \simeq \frac{K\omega\tau C_A \circ 2\mu}{K_s(\sigma_c+\sigma_{ic})(\mu_e + \mu_f)}$$

It may be helpful to note that

$$\mu_f \simeq \mu_{ic} > \mu_e$$

However, τ , σ_c and σ_{ic} depend strongly upon the energy of the incident photons and the atomic number of the elements. In the range of 0-80 keV, $\tau > \sigma$ (where $\sigma = \sigma_c + \sigma_{ic}$) for heavier elements whereas σ is in order of τ for lighter elements. By using Si(Li) or Ge(Li) detector, $k_s >> k$ may be possible.

The intensity and the energy of the incoherent scattered photon depend on their scattering angles. As the scattering angle increases, the energy of scattered photon decreases. At a scattering angle of 180°, the energy of scattered photons is reduced to a minimum whereas the minimum intensity occurs at 90°. In practice, the intensity of the incoherent scattered peak can be minimized by positioning the detector at 90° with respect to the direction of primary X-ray beam.

Apart from the fluorescent X-ray peaks, the following peaks can also be seen in the spectrum:

- coherent scattered peak with energy equal to that of the primary photon.
- incoherent scattered peak with its energy peak equal to

$$E' = \frac{E}{1 + \frac{E}{511}(1 - \cos\theta)}$$

where E' is the energy of the primary photon in keV,

E is the energy of the incident scattered peak in keV, and

θ is the scattering angle.

It should be noted that the incident scattered peak is broader comparing other peaks. This is because of the energy distribution of incoherent scattering of primary photons through different angles.

- escape peaks resulting from escaping of characteristic X-ray of the detector materials i.e. Si X-ray for Si(Li) detector, Ge X-ray for Ge detector, Xe X-ray for Xe-filled detector and so forth. As a result, there also are escape peaks at the lower end of the spectrum which are separated from the parent lines and appear at the energies of E_{parent} less the energy of Si K , Ge K , Xe L , etc., accordingly. This only happens when energy of the photon is greater than the absorption edge of the detector material. Take the case at E_{parent} = 20 keV, the escape peak energies will appear at for

- Si(Li) detector E = E_{parent}-Si K = 20 - 1.740 = 18.260 keV,
- Ge detector E = E_{parent}-Ge K = 20 - 9.885 = 10.115 keV, and
- Xe-filled detector E = E_{parent}-Xe L = 20 - 4.111 = 15.889 keV.

These escape peaks may interfere or overlap lower energy peaks resulting in difficulties and errors in qualitative and quantitative analysis. Fig. 2.5 shows a spectrum of Nb K X-rays with their escape peaks including escape peaks of coherent and incoherent peaks (detected with HPGe detector).

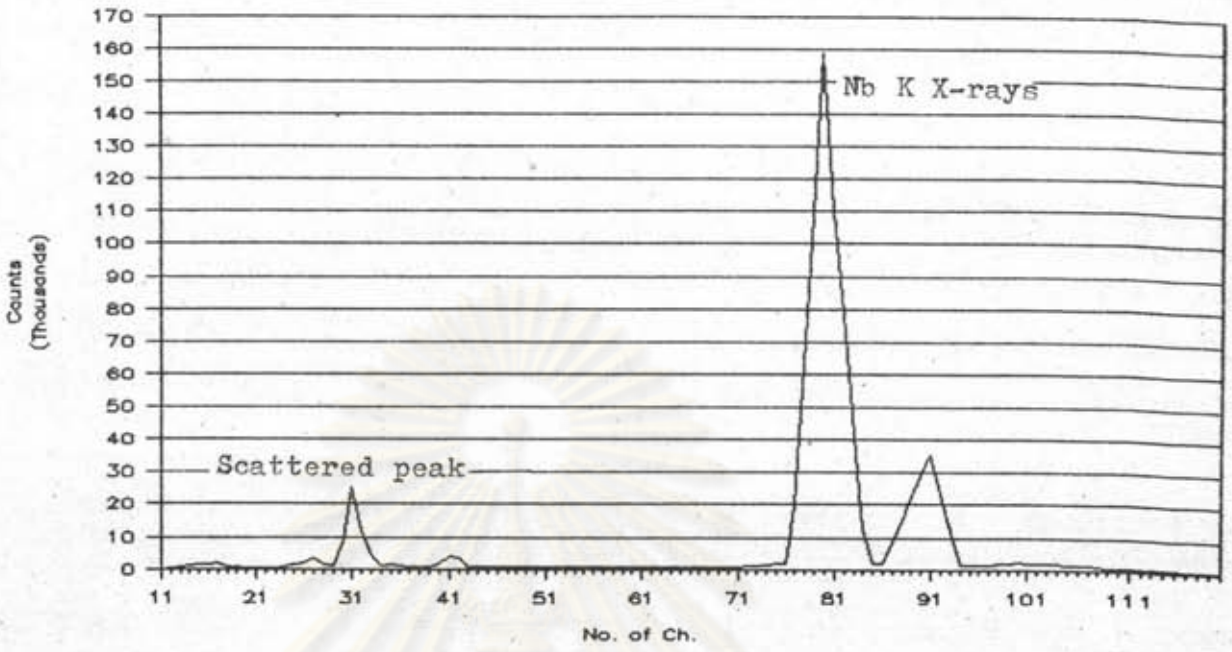

Fig. 2.5 Spectrum of Nb K X-rays showing the scattered peaks of primary photons from Cd-109 source detected with HPGe detector.

2.3.2 Radioisotope X-Ray Sources.

In wavelength dispersive spectrometer, the fluorescent X-rays of the specimen are stimulated by high intensity X-ray tube and detected with the help of a diffracting crystal-goniometer-collimator system. For energy dispersive spectrometer, the specimen can be stimulated by a radioisotope source or an X-ray tube hence its secondary

fluorescent X-rays will be detected directly with a suitable detector, without a diffracting crystal as illustrated in Fig. 2.6

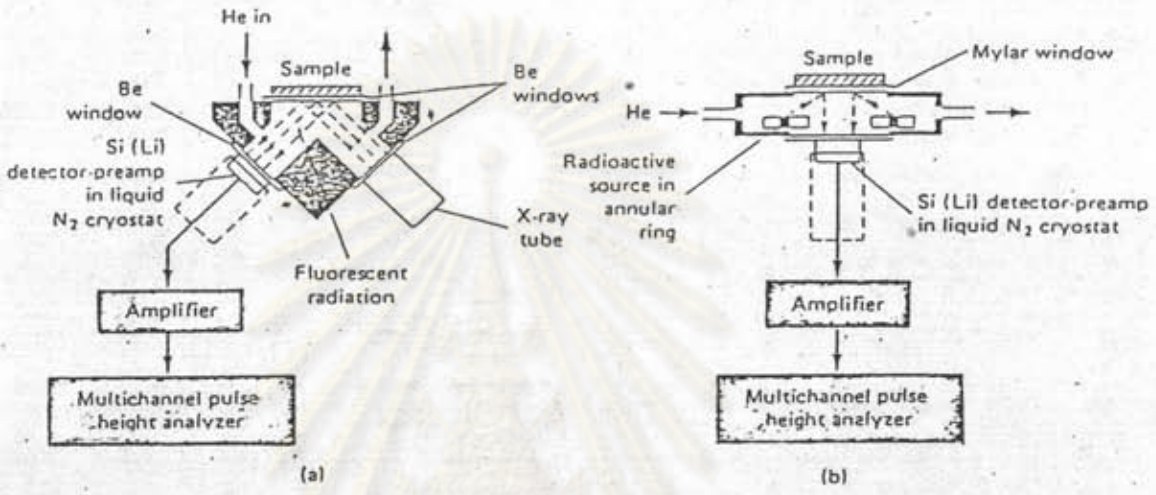

Fig. 2.6 Energy dispersive X-ray spectrometer. Excitation by X-rays from (a) a tube and (b) a radioactive source.

In this research, only a radioisotope excited energy dispersive X-ray (EDX) spectrometer, is designed, constructed and tested for analysis of sulfur and lead in fuel oils. There are a lot of reasons for that choice. Firstly, its speed is over the wavelength dispersive spectrometer, secondly

it can measure all expected and unexpected elements, thirdly it can display the data and ease the interpretation, fourthly there are only a fewer geometric constraints and finally it is lower cost; moreover, its composing instruments can be sought easily for the measurement.

The following components are decisive for radioisotope X-ray spectrometer;

(1) the radioisotope source for the excitation of characteristic X-rays,

(2) the detection system for isolating secondary X-rays and for measuring the intensity of the isolated X-rays of an element,

(3) the sample-source-detector geometrical arrangement which has to secure an efficient use of the radiation.

In table 2.2, the X-ray and gamma-emitting sources used in the EDX analysis are given. For an efficient excitation of the characteristic X-rays of elements sought in a sample and for their identification, the following rules may be useful:

Firstly, for a multielement analysis, the energy of the exciting X-ray or gamma-ray must be above the energy of

the K or L absorption edge of the interesting elements which are characterized by energies from 1.0 keV to 98 keV (corresponding to the K absorption of Na with atomic number Z = 13 to U with Z = 92) and 2 keV to 20 keV (corresponding to the L absorption of Zr with Z = 40 to U, also seeing in Table 1), respectively. In order to avoid an overlap of K X-lines by L X-lines of heavy elements, the exciting source should be adapted to the K absorption edge of the element with the highest atomic number of the sample if for this element Z<40. Moreover, because the efficiency of excitation of an element decreases with an increasing energy gap between the absorption edge and the photon energy of the source for multielement analysis, the selection of several sources may be advantageous and should be taken into consideration.

Secondly, in selecting excitation sources, a careful test on the purity of the X-ray or gamma-spectrum emitted from radioisotopes which are encapsulated above all in annular or point source is necessary.

Finally, isotope-excited X-ray fluorescence spectra are characterized by a high background, i.e. lines at energies other than the characteristic lines, resulting above

all from radiation scattered from the sample and from components of the measurement assembly. The scattered photons of the exciting primary photons may constitute a large part (up to 99%) of the observed counts. The scattering background also includes the coherent and incoherent scattering.

In summary, for the practical use of commercial and, above all, specially developed radioisotope X-ray fluorescence system, a careful selection of exciting sources or source target arrangement, is important. Moreover, above all the influence of the backscattered photons of the exciting source photons must be carefully determined and efforts made for a reduction of backscatter interference as much as possible.

Table 2.2 : Exciting Sources.

Source	mCi	Geo-metry*	Decay mode**	Half-life	Emission, keV	Yield, % per disintegra-tion	Element coverage, atomic number
^{55}Fe	50	A	EC	2.7 a	5.9[MnK]	26	9 – 24
^{55}Fe	25	D					
^{109}Cd	5	A	EC	453 d	22.1[AgK]	107	20 – 43
^{109}Cd	3	D			87.7[γ]	4	
^{241}Am	60	A	α	458 a	59.6[γ]	36	
^{241}Am	10	A			14–22[NpL]	37	28 – 69
					26.4[γ]	40	
^{238}Pu	30	D	α	86.4 a	12–17[UL]	10	23 – 38 56 – 82
					144[γ]	9.7	
^{57}Co	10	A	EC	270 d	136[γ]	11.1	70 – 98
					122[γ]	85.2	
					6.4[FeK]	51.0	

*A – annular source;
D – disc source.
**EC – electron capture.

2.3.3 X-Ray Detectors

Techniques for XRF analysis are based on the use of solid-state, scintillation and proportional detectors. The techniques are different for each type of detectors because of their large differences in resolving power for X-rays (Fig. 2.7 and 2.8).

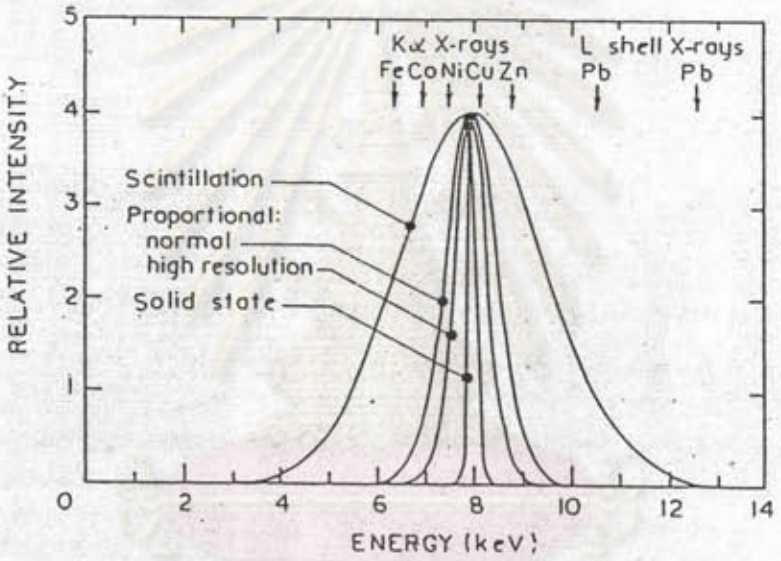

Fig. 2.7 Resolution of X-ray detectors for Cu K_α X-rays illustrated in relation to energies of fluorescent X-rays of some elements commonly determined in on-stream analysis.

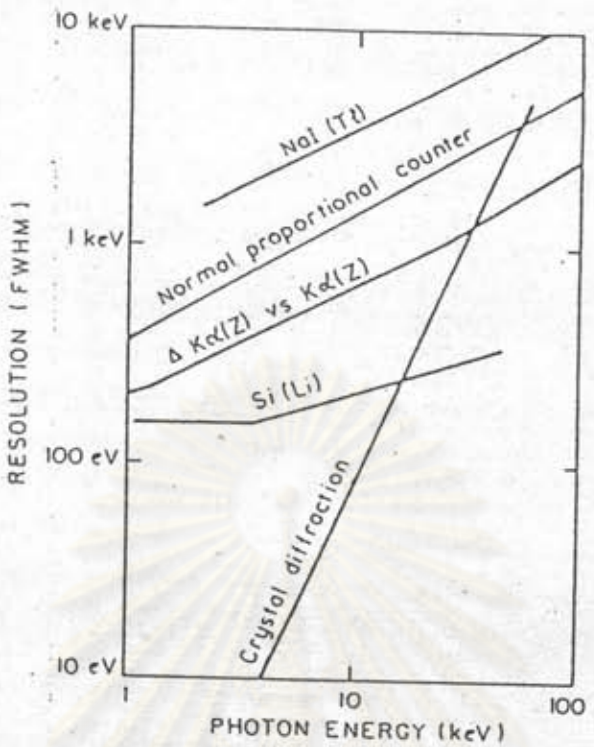

Fig. 2.8 Energy resolution of detectors and adjacent element K X-ray peak separation.

Solid-state detectors resolve K X-rays from elements of adjacent atomic number (Z), hence element concentration is obtained by simple signal processing. Proportional counters (high resolution) have worse resolving power which results in some spectral processing is required. Scintillation detectors cannot resolve adjacent Z elements so analysis combines coarse spectral analysis to separate fluorescent from backscattered X-rays with the use of X-ray filters to isolate the K X-rays.

(1) XRF Analysis Using Solid State Detectors

Solid-state detectors are mainly used to analyse mineral sample in laboratory, but they are in limited use for on-stream analysis. The main advantage is that their high resolution enable simultaneous multielement analysis with excellent sensitivity. Minimum detectable levels are, for Z>24, about 20-50 parts per million (ppm). Analysis for low Z elements, e.g. silicon and aluminium, is also possible but considerable sample preparation is essential to ensure homogeneous samples.

(2) XRF analysis using scintillation detectors

Scintillation detectors have found many applications in the field, in industrial plants and in the laboratory for routine quantitative and semi-quantitative determination of minor and major elements in a wide range of solids and liquids such as ores, metals and solutions. The advantages of XRF analysis using scintillation detectors are that the sensitivity is adequate for many practical applications, minimum detectable levels for very favourable cases can be as low as 50 ppm, but usually they are in the

range 100 to 300 ppm. Multielement analysis is probably unpractical because it would require a mechanically complex filter changer with two filters for each element to be determined.

(3) XRF analysis using proportional detectors

Recent developments is proportional detectors have led to a moderate improvement in X-ray resolution. Energy resolution is now sufficient to enable adjacent elements to be measured simultaneously if their concentrations are similar. In practice, counts between the FWHM (Full width at half maximum) of the fluorescent X-ray spectral peaks are measured and corrections made for the overlap X-ray peaks from adjacent elements. Correction for sample matrix absorption are made using the measured intensity of back scattered X-rays.

The above system can be used for the simultaneous determination of up to about four close Z elements. Sensitivity and accuracy are about the same as for scintillation detectors for elements of Z>25, and considerably better for lower Z elements.

2.3.4 Quantitative Analysis with XRF Technique

According to

$$I_f = K \frac{C_A}{\mu_e + \mu_f}$$

The relationship between the fluorescent intensity of an X-ray peak and concentration of an element (C_A) is usually not linear in thick layers due to matrix absorption (μ) or enhancement effects. However, in the range of low concentrations a linear calibration function can generally be obtained which is suitable for the determination of the detection limit.

There are various techniques for quantitative analysis such as the calibration method, the dilution method, the standard addition method and the internal standard method in order to overcome the matrix effects. In this research, it will only refer to the calibration method.

Calibration Against Standards.

Here, the relationship between the analytical line intensity and the concentration is determined empirically with a set of standards that closely approximate the samples overall composition. This technique is applicable only when the absorption and enhancement effects are identical for both samples and standards.